Int. J. Electrochem. Sci., 11 **(2016)** 10185 – 10198, doi: 10.20964/2016.12.32

International Journal of ELECTROCHEMICAL SCIENCE
www.electrochemsci.org

Corrosion Studies of Carbon Steel Immersed in NACE Brine by Weight Loss, EIS and XRD Techniques

Román Cabrera-Sierra[1,2*], *L. J. Cosmes-López*[1], *Homero Castaneda-López*[2,3], *Jesús Torres Calderón*[1], *J. M. Hallen López*[4]

[1] Instituto Politécnico Nacional, Escuela Superior de Ingeniería Química e Industrias Extractivas. Departamento de Ingeniería Química Industrial, Edif. 7, UPALM Zacatenco, México, D.F. C.P. 07738.
[2] Chemical and Biomolecular Engineering Department, The University of Akron, Akron, Ohio 4325, USA.
[3] National Corrosion Center, Material Science and Engineering Department, Texas A&M University. College Station, TX 77843.
[4] Instituto Politécnico Nacional, Escuela Superior de Ingeniería Química e Industrias Extractivas. Departamento de Metalurgia y Materiales, UPALM Zacatenco, México, D.F. C.P. 07738.
[*]E-mail: romaipn@gmail.com

Received: 28 June 2016 / *Accepted:* 22 September 2016 / *Published:* 10 November 2016

Weight loss and corrosion rate measurements were determined by the immersion of the carbon steel for 24 hours in NACE brine; varying the rotation speed (200, 1000 and 2000 rpm) and the temperature (35, 50 and 65 ^{o}C). At this immersion time, the steel interface was further characterized by Electrochemical Impedance Spectroscopy technique (EIS), using the rotating cylinder electrode configuration. It was observed an increase in the oxidation of the steel by influence of the rotation mainly at temperatures of 50 and 65 ^{o}C; the corrosion rates increase from 25.99 to 110.52 and 45.2 to 135.27 mpy, respectively. This active oxidation is evident in the EIS characterization recording a shrinkage of the complex plots as the rotation and temperature were enhanced. According to the EIS analysis the electrochemical responses are governed by the oxygen diffusion process through the corrosion products under the influence of the electrode rotation. Using XRD analysis, the iron compounds formed by oxidation - precipitation after the immersion are mainly composed by magnetite (Fe_3O_4) and feroxyhyte (δ-FeOOH), respectively; being the feroxyhyte partially removed by the rotation favoring the active dissolution of the steel.

Keywords: Corrosion, EIS, brine, RCE

1. INTRODUCTION

It is well known that the internal corrosion process in pipelines is mainly due to the corrosive brine transported along with the oil [1-3]; whose percentage (water cut) enhances the corrosion rate

[4]. In the oil industry, control of the corrosion process is achieved by dosing corrosion inhibitors such as amines, amides, imidazole, among others [3,5,6]. Previous to their application, they are evaluated in laboratory using different methods such as: wheel test, cylinder electrode, rotating cylinder electrode and/or rotating cage, among others [7,8]. With the exception of the wheel test, these techniques are used to evaluate the corrosion process under different flow conditions (based on Reynolds number) simulating operating pipelines.

It has been established that the corrosion inhibitors should be evaluated using similar conditions as those found in pipelines; however, it is difficult to mimic the corrosive media and/or the presence of corrosive gases. Hence, it is important to analyze the chemical composition of different brines transporting the hydrocarbon phase, in this case from the South of Mexico. According to these analyses, high salinity values above 40 % have been determined reaching acid pHs (below 5) and/or in the presence of corrosive gases (H_2S, CO_2). Taking into account these results the NACE 1D182 [9] brine is adopted for evaluating the corrosion process of the steel, determining the inhibitor behavior of different chemical compounds and/or the selection of corrosion inhibitors. The benchmark of this investigation is studying the corrosion process of 1018 carbon steel immersed in a brine solution to consider pipelines transporting water cuts above 85 % in field.

Thus in this work, different corrosion studies using the NACE brine described in ref [9] varying the rotation speed and temperature are performed, using the rotating cylinder electrode configuration. The aim of these studies is identifying the corrosiveness of the brine in absence of corrosive gases by using weight loss (WL), electrochemical impedance spectroscopy (EIS) and X-ray diffraction (XRD) techniques. These results are important when electrochemical probes are used for on line monitoring corrosion rates in field and/or evaluating different corrosion inhibitors. Furthermore, in a forthcoming publication the corrosiveness of the brine in presence of corrosive gases will be addressed in order to establish the influence of CO_2 or H_2S during the steel oxidation.

2. EXPERIMENTAL SECTION

A rotating cylinder electrode configuration to perform gravimetric and electrochemical measurements was used after the immersion of the steel for 24 hours. The experiments were conducted in a conventional three electrode cell (200 mL), using a silver/silver chloride electrode Ag/AgCl (0.235 V vs. SHE) as reference and introduced into a Luggin capillary. The rotating cylinder electrodes (RCE) were 12 mm in diameter and 7.96 mm in length (aprox. 3 cm^2) made of 1018 carbon steel and the auxiliary electrode was a graphite rod. The NACE 1D182 brine had the following chemical composition: 9.62 % NaCl, 0.305 % $CaCl_2$, 0.186 % $MgCl_2.6H_2O$ and 89.89 % doubled distilled water [9]. This aqueous solution was non deaerated containing 6 to 8 ppm of oxygen approximately. The corrosion studies were performed two times varying the temperature (35, 50 and 65 ^oC) and the rotation rate of the electrode (200, 1000 and 2000 rpm). The temperature was controlled using a recirculating bath.

Weight loss measurements were recorded until a variation of 0.1 mg during the cleaning (removal of corrosion product) of the samples, using an analytical balance. The cylinder electrodes

were mechanically polished using SiC emery papers in the following order: 240 and 400 until obtaining homogeneous surfaces and rinsed with alcohol. After the immersion the steel cylinders were chemically cleaned using an inhibited hydrochloric acid [10].

After the immersion tests, the open circuit potential (OCP) was recorded as were the EIS characterization using an amplitude of 10 mV vs the corrosion potential using a GAMRY potentiostat – galvanostat. The frequency was varied from 100 kHz to 0.01 Hz at 10 points per decade. The EIS diagrams were fitted by means of equivalent circuit and the non linear regression algorithm developed by Boukamp [11].

XRD was used to determine the iron phases formed on the carbon steel after its immersion in the NACE solution, using a diffractometer with Cu Kα radiation. A range from 20° to 120° was scanned with a step width of 0.02°. The qualitative analysis of the XRD spectra was carried out using commercial software.

3. RESULTS AND DISCUSSION

3.1. Gravimetric measurements

In order to evaluate different corrosive conditions of the steel immersed for 24 hours in the NACE brine, the weight loss measurements were recorded varying the rotation speed of the cylinder and the temperature. The WL values at 35 ^{o}C were 0.00433, 0.00657 and 0.0093 grams and rotation rates of 200, 1000 and 2000 rpm, respectively; meanwhile for 50 and 65 ^{o}C, for the same rotations, the values were: 0.0041, 0.0126, 0.0172 and 0.0071, 0.01643 and 0.0203 grams. According to these results, the steel oxidation is enhanced by the temperature and rotation of the electrode; being one order of magnitude larger for 50 and 65 ^{o}C than those recorded at 35 ^{o}C. Besides, during the immersion tests, a dark colored surface was evident on the entire steel when the oxidation is moderate (e.g. 35 ^{o}C); meanwhile whether the oxidation is augmented (e.g. 50 and 65 ^{o}C), a red color film seems to be externally formed covering most part of the surface. It is assumed this film is likely formed by precipitation with poor adherence because it is easily detached from the steel surface by influence of the rotation favoring the oxidation of the steel.

Based on these results and the specifications of the carbon steel cylinders (density 7.86 g/cm^3), the corrosion rate in mills inch per year (mpy) were calculated and shown in Figure 1. As can be seen the minor corrosion rates are obtained at 35 ^{o}C varying from 28.52 to 61.37 mpy as a function of the rotation speed; followed for the temperatures at 50 and 65 ^{o}C, reaching values from 25.99 to 110.52 and 45.2 to 135.27 mpy, respectively. These corrosion rates at 50 and 65 ^{o}C and 1000 and 2000 rpm can be related with a rapid dissolution (active condition) of the steel in the Brine solution.

It seems that the corrosion rate of the steel increases linearly as a function of the temperature and the rotation; this increase is minor for 35 ^{o}C (slope 0.0183), meanwhile for 50 and 65 ^{o}C the slopes recorded are similar (~0.048); being very corrosive towards the steel. It is presumed that once the electrode is rotated there is a decrease in the thickness of the corrosion films and the diffusion of aggressive species (e.g. oxygen) is enhanced raising the dissolution of the steel and the likely

precipitation of iron compounds at the film – solution interface. Under these conditions, the dissolution of the steel could be similar for 1000 and 2000 rpm, however the mobility of different species (iron ions and oxygen) through the corrosion films is favored as the temperature increases.

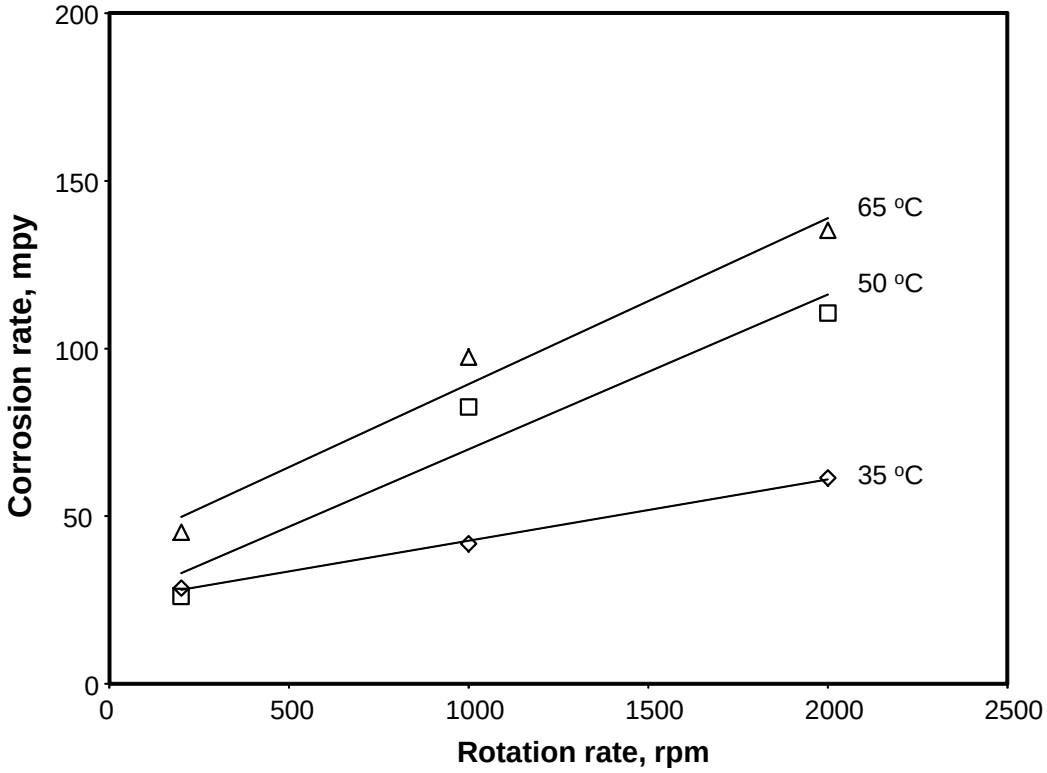

Figure 1. Corrosion rate measurements of carbon steel immersed after 24 hours in NACE solutions using a Rotating Cylinder Electrode configuration.

3.2. Electrochemical studies

3.2.1. Open circuit potential measurements

After the immersion of the steel for 24 hours in the NACE solution, the open circuit potential was recorded and plotted in Figure 2. It is interesting to note that for each temperature the potential becomes positive almost 50 - 54 mV as the rotation speed is raised at 2000 rpm, except for 65 ^{o}C; meanwhile, the potentials seems to be very similar for each rotation rate. These variations in the open circuit potential could be related with minor modifications at the film – solution interface, e.g. an increase in the dissolution of the steel, precipitation of different iron compounds and/or a decrease in the thickness of the corrosion films by the rotation. All these phenomena may be occurring simultaneously during the steel oxidation which shown an active condition as the potential becomes positive, enhancing its oxidation (see Figure 1).

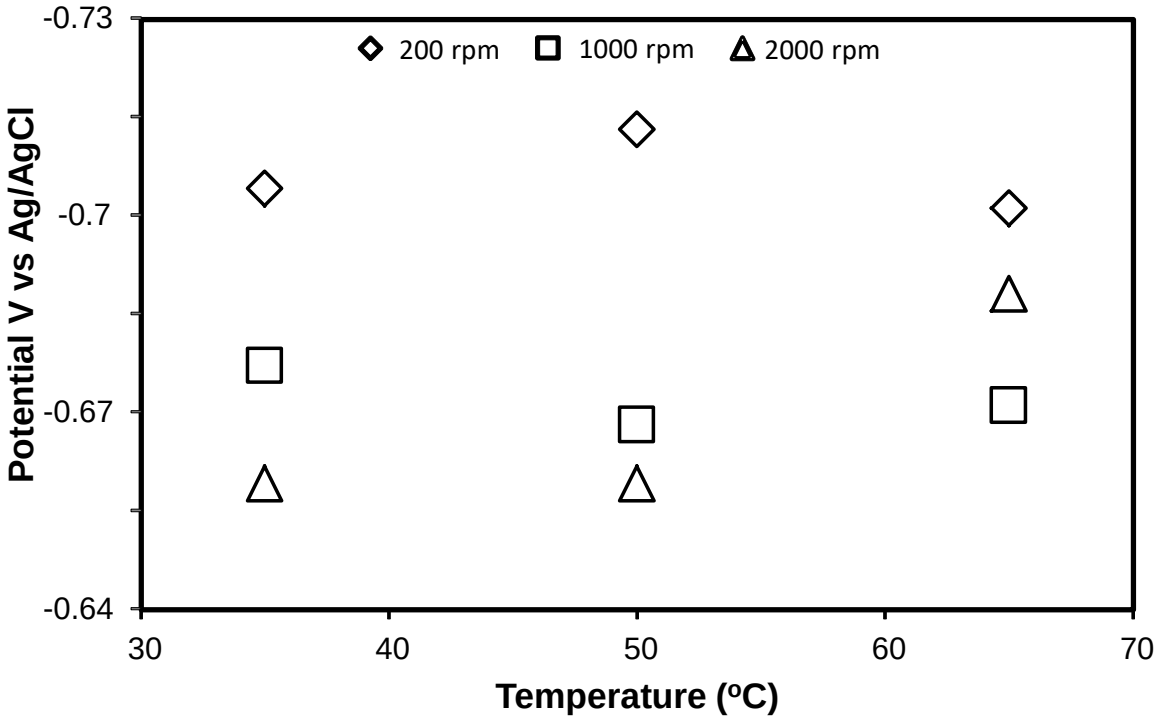

Figure 2. Corrosion potential measurements after 24 hours of immersion of carbon steel in NACE media using a Rotating Cylinder Electrode configuration.

3.2.2. EIS characterization

In Figures 3 – 5 are displayed the EIS diagrams of the steel immersed in the NACE solutions. In these figures, important variations in the impedance values (mainly Nyquist plots) are recorded, as a result of the steel oxidation depending on the temperature and rotation of the electrode.

At the lower temperature (35 ^{o}C), Figure 3, the complex plots exhibit a capacitive behavior related with the presence of semicircles which decreases in diameter from 200 to 100 ohms as the rotation increase from 200 to 2000 rpm (Figure 3a); however, the plot at 1000 rpm is slightly modified because the appearance of a second loop at low frequencies. The reduction in the impedance values by influence of the rotation can be related with a conventional diffusional process occurring from the bulk solution to the interface, through the corrosion products or both. Conversely to the Nyquist plots, the Bode diagrams (Figure 3b) are less sensitive with the rotation of the steel. In this Figure, the capacitive responses are dominant from intermediate to low frequency regions which are similar for 200 and 1000 rpm; meanwhile for 2000 rpm the appearance of two maxima at intermediate frequencies (~10 Hz) is observed. In this regard, the phenomena involved in the oxidation of the steel are influenced by the rotation of the electrode.

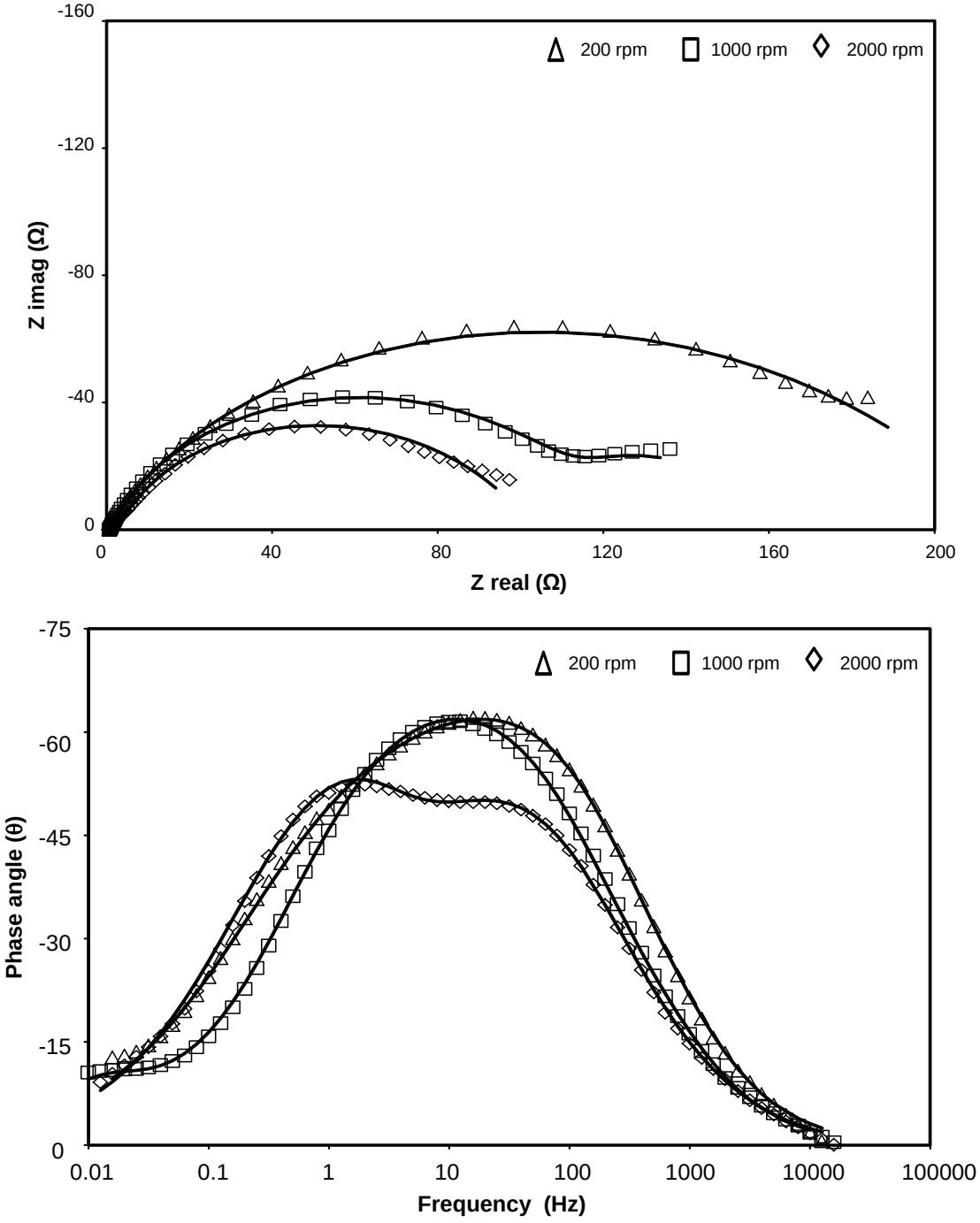

Figure 3. EIS diagrams recorded after 24 hours of immersion of carbon steel in NACE media at 35 ^{o}C using a Rotating Cylinder Electrode configuration. The continuous line represents the fit obtained using the Boukamp program.

When the temperature is increased at 50 and 65 ^{o}C (Figures 4 and 5), similar complex and Bode diagrams are displayed than those shown in Figure 3. In the former, the semicircle responses decrease in diameter reaching impedance values less than 70 Ω (Figure 4a) and 50 Ω (Figure 5a), as a function of the rotation rate; these modifications in the complex plots can be related with an increase in

the active oxidation of the steel, favoring its dissolution, the formation of iron ions (Fe^{+2} and/or Fe^{+3}), its diffusion and the likely precipitation of iron compounds.

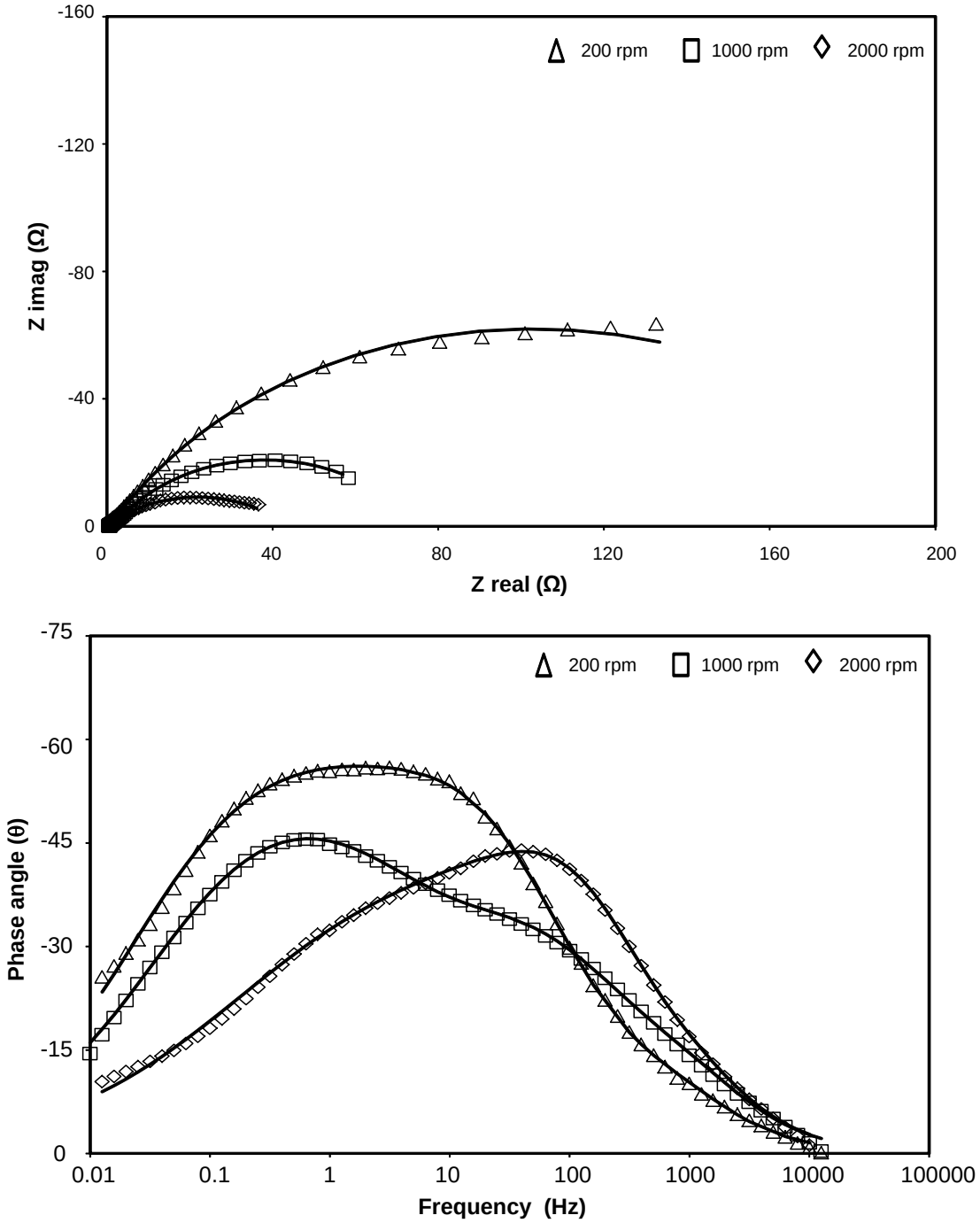

Figure 4. EIS diagrams recorded after 24 hours of immersion of carbon steel in NACE media at 50 ^{o}C using a Rotating Cylinder Electrode configuration. The continuous line represents the fit obtained using the Boukamp program.

In the other hand, minor modifications are detected in the Bode diagrams when the temperature is increased; e.g., it can be noticed a decrease in the phase angle values at 200, 1000 and 2000 rpm in Figures 4 and 5. Also as the rotation increased, the capacitive response observed for 200 rpm split in

two maxima phase angles for 1000 and 2000 rpm at intermediate frequencies. The maxima detected at 100 and 1 Hz are enlarged for 2000 and 1000 rpm, respectively. Taking into account these capacitive responses, it can be considered they are related with diffusion processes which are controlling the oxidation of the steel under the influence of the rotation rate. Similar findings are evident in Figure 5 when the temperature is 65 ^{o}C, except that the maxima phase angles are less defined from intermediate to low frequencies regions.

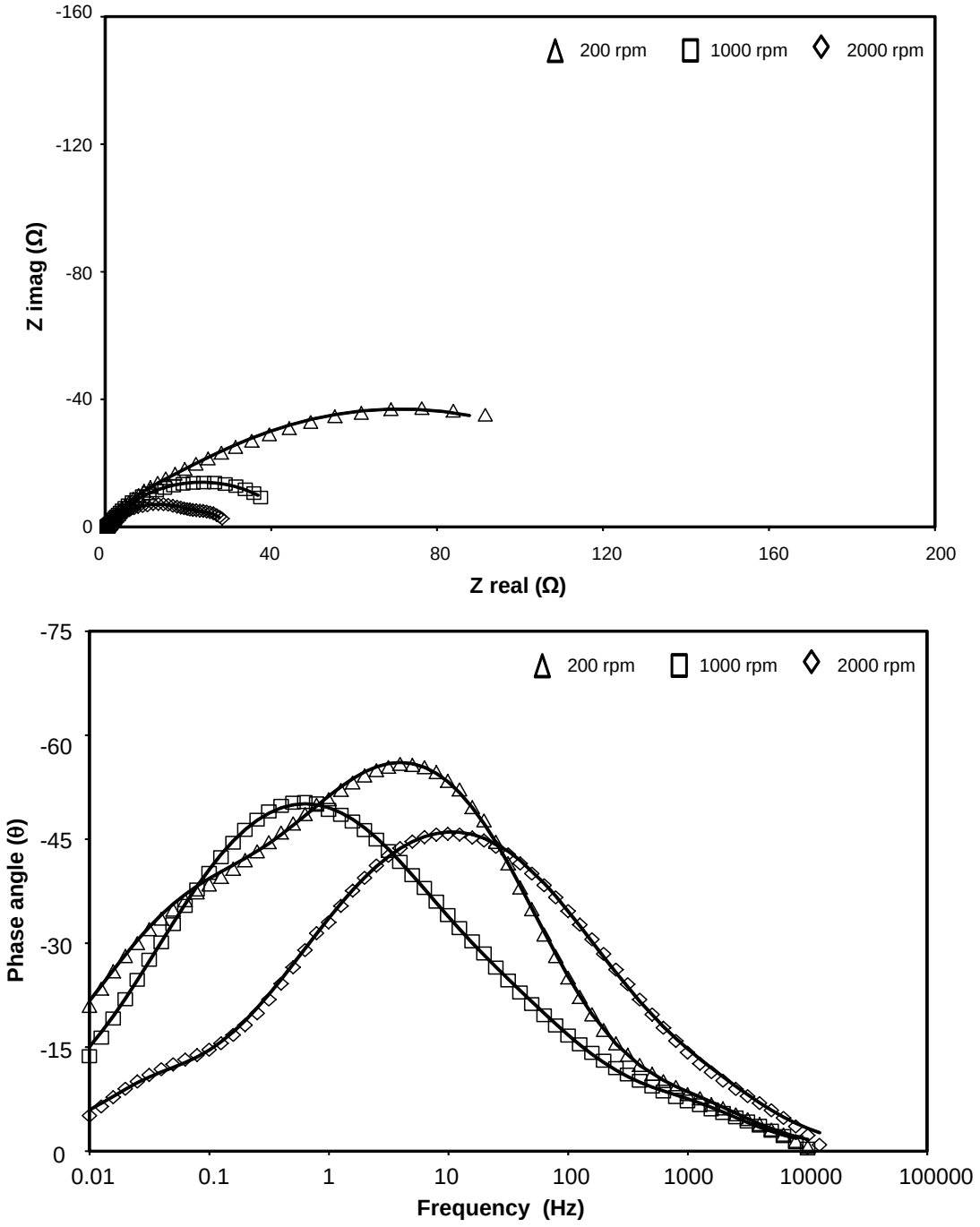

Figure 5. EIS diagrams recorded after 24 hours of immersion of carbon steel in NACE media at 65 ^{o}C using a Rotating Cylinder Electrode configuration. The continuous line represents the fit obtained using the Boukamp program.

Based on these diagrams, the rotation speed favored the oxidation of the steel in major extent than the temperature raising the sensitivity of the EIS technique and its beneficial application in field measurements.

In specialize literature studying the corrosion process of mild steel in sour or aerated environments [12-19], different diffusion process that could be occurring through the corrosion films had been reported; e.g. iron ions from the metal to the aqueous solution and/or the oxygen gas from the electrolyte to the carbon steel interface. In the first case, the iron ions could be diffusing by interstitial [20-23] through the oxide forming iron compounds by precipitation; meanwhile, the diffusion of oxygen through the films is for considering the reduction reaction on the steel and the likely precipitation of hydroxides [14-19]. It is presumed the diffusion of the iron ions is favored by the temperature and/or rotation, meanwhile the oxygen is mainly introduced by rotation until the film – solution interface; being this diffusion process retard whether this specie diffuse through the corrosion films. Hence it can be considered these diffusion phenomena during the characterization of the steel by EIS technique and related with the formation of two maxima phase angles in the Bode plots. Furthermore the contribution of the steel oxidation at the metal – film interface can be considered in the simulation of the EIS diagrams.

Figure 6 sketches the equivalent circuit describing the corrosion process occurring in three simultaneous steps in the following way: Rs is the solution resistance (Ω), C_f is the corrosion product layer capacitance (μF) and Rct is a charge-transfer resistance at the metal-corrosion products interface (Ω). R_{dif1} and Q_{dif1} is an electrical arrangement to describe Fe^{2+} ion diffusion through the oxide film, which is the most plausible phenomenon to account for the iron compounds formed externally on the steel surface. To extrapolate the low-frequency diffusion impedance, R_{dif2} and Q_{dif2} are associated with the molecular oxygen diffusion process typical of aerated solutions [14-19]. The fitting obtained in Figures 3 to 5 is represented by the continuous line using the equivalent circuit program developed by Boukamp [11]. In these Figures it can be observed a reasonable fitting (Chi-Sqrd: 10^{-5}) and the parameters obtained are indicated in Table 1.

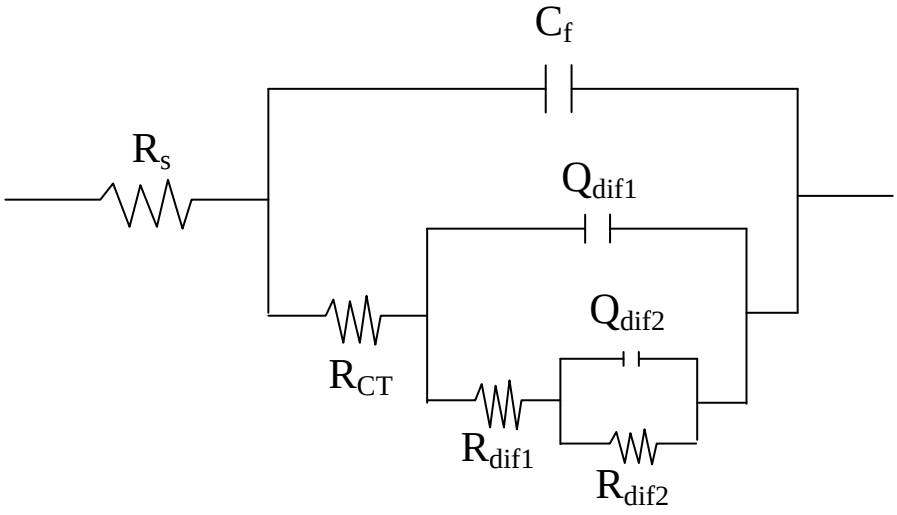

Figure 6. Equivalent circuit used for fitting the EIS diagrams using the Boukamp program.

Table 1. Parameter values obtained after the fitting of the EIS diagrams using the Boukamp program.

Temperature	Rotation rate (rpm)	R_s (Ω)	C_f µF	R_{CT} (Ω)	Q_{dif1} (siemens) $Y_0 \times 10^2$		R_{dif1} (Ω)	Q_{dif2} (siemens) $Y_0 \times 10^2$		R_{dif2} (Ω)
35 °C	200	0.7	413.5	0.68	0.23	0.74	22.14	0.27	0.53	196.25
	1000	0.88	466.6	0.73	0.35	0.72	121.5	49.33	1	30.31
	2000	0.66	542.2	0.19	0.80	0.67	20.42	0.28	0.94	81.91
50 °C	200	0.65	872.3	0.26	1.07	0.755	15.62	0.874	0.62	189.65
	1000	0.6	545.5	0.26	1.625	0.653	4.07	2.07	0.67	69.49
	2000	0.62	521.4	0.429	0.21	0.843	2.31	2.41	0.50	40.64
65 °C	200	0.63	812.4	0.172	1.483	0.761	34.27	3.55	0.68	96.41
	1000	0.6	990.0	0.143	3.16	0.713	1.71	2.66	0.71	43.06
	2000	0.56	465.24	0.184	1.681	0.645	24.66	143.22	1	38.95

The solution resistance is in the same order of magnitude (less than 1 Ω) and slightly decreases when the rotation rate and temperature are enhanced; this variation in the conductivity of the brine can be related with the dissolution of the steel depending on the temperature and rotation of the electrode.

In order to discuss the semiconductor properties of the corrosion films formed on the steel, the capacitance element can be related with modifications in the chemical composition and/or thickness of the corrosion films. In the former, when exist the formation of iron oxides and sulfides with a porous nature, capacitance values in the order of mF had been reported [13-16]; meanwhile for resistive passive films, these values are less than 100 µF [24-26]. In table 1, it can be observed values from 413.5 to 542.2 µF for 35 °C as a function of the rotation rate, conversely, the capacitance decreases for 50 and 65 °C. In general these results are less than 1 mF, indicating the likely formation of iron oxides with a porous nature. As a robust approximation, a minor thickness by the rotation of the electrode is expected accompanied with an increase in the capacitance. This assumption could explain the maximum capacitance values recorded at 35 °C at 2000 rpm; unlike this temperature the results obtained at 50 and 65 °C can be explained considering the likely formation of different corrosion products, instead of commonly iron oxides (see below).

To describe the oxidation of the steel, the resistances (R_{CT}, R_{dif1} and R_{dif2}) obtained by the simulation of the EIS diagrams can be analyzed. The R_{CT} term shown the minor values decreasing from 0.68 to 0.143 Ω, as the temperature and the rotation rate increased; likely related with the steel oxidation. According to these results, this oxidation is rapid however the diffusion of different species through the corrosion films controlled its corrosion rate; likely due to the interstitial iron ions (R_{dif1}) and molecular oxygen (R_{dif2}) diffusion [12-19]. In one hand, the R_{dif1} element seems to be similar varying the rotation of the electrode at 35 °C; meanwhile for 50 and 65 °C, these values decrease. This means that depending on the corrosion products formed on the steel and its thickness, the diffusion of iron ions is influenced for rotations at 1000 and 2000 rpm; it is presumed the formation of stable iron oxides adhered to the steel for 35 °C being less removed for these conditions. At 50 and 65 °C it seems that the semiconductor properties of the corrosion films are different, because the R_{dif1} element decreases as a function of the temperature and rotation; except the resistance obtained at 2000 rpm and 65 °C. To explain these results the likely formation of different iron compounds on the steel surface is considered, e. g. hydroxides or oxy-hydroxides by precipitation; because they are easily detachment

from the steel surface. Thus a decrease in the thickness is expected, enhancing the ingress of corrosive ions, the diffusion of iron ions and the precipitation of oxy-hydroxides on the steel electrode (active oxidation).

In the other hand, the oxygen diffusion is influenced because the rotation and temperature. This hypothesis is supported by considering the variation of the R_{dif2} term in Table 1. It is observed a decrease in this resistive element as a function of the temperature and in major extent by the rotation of the electrode. The minor values obtained were 40.64 and 38.95 Ω at 2000 rpm at 50 and 65 ^{o}C, respectively. Taking into account these results the diffusion of the oxygen until the steel is occurring at the same rate; however the corrosion rates are larger for 65 ^{o}C (see Figure 1). Furthermore, these experimental conditions are the most aggressive during the immersion of the steel (see Figure 1) in the NACE solution; this mean that the diffusion of molecular oxygen through the iron compounds is controlling the corrosion rate of the steel varying the temperature and the rotation of the electrode.

Based on the corrosion rates determined by weight loss and the resistance (R_{dif2}) values related with the controlling step in the oxidation of the steel, the corrosion current density and the Tafel constant (β) can be calculated. The current density varied from 56.83 - 295.8 μA/cm^2 supporting the active dissolution of the steel as a function of the temperature and rotation; meanwhile the B values are less sensitive with an average of 0.0312 V or 31.2 mV. It is noteworthy this B value for on line monitoring corrosion rates using electrochemical probes, because conservative values in the order of 22 mV had been reported [27]; being slightly minor in comparison with those calculated using weight loss measurements.

3.3. XRD studies

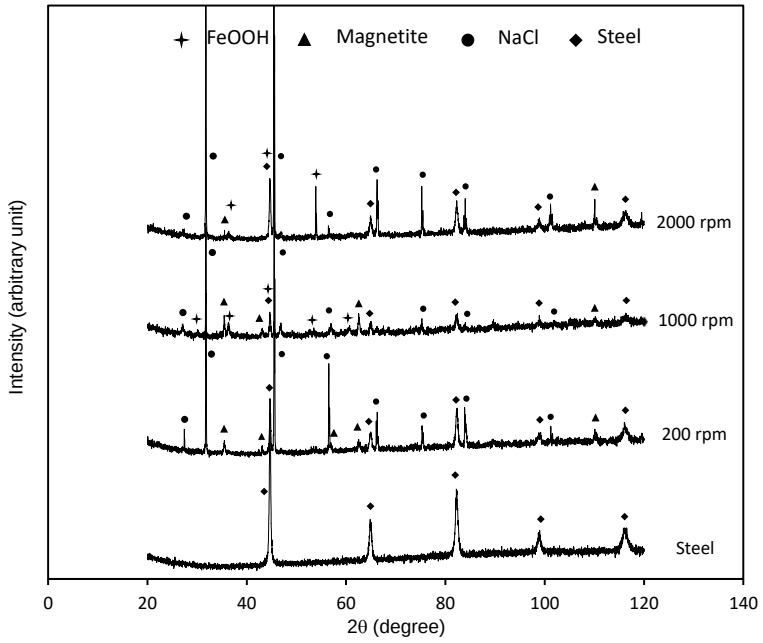

A

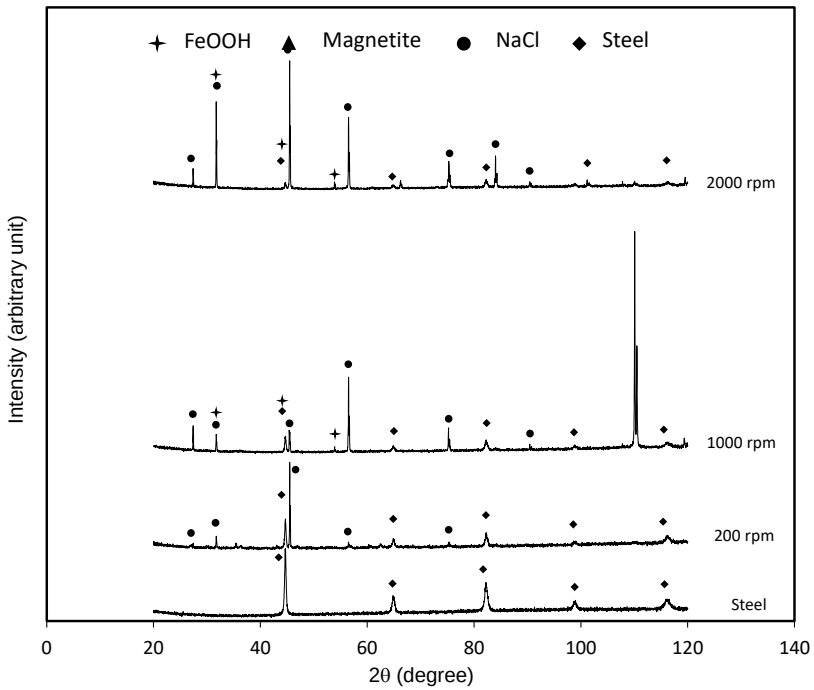

B

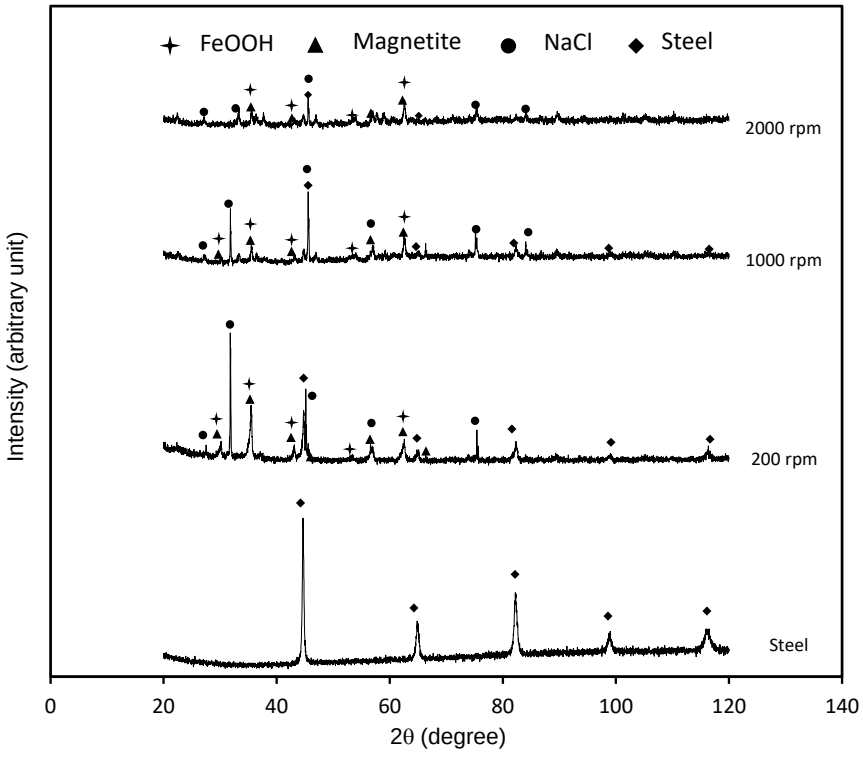

C

Figure 7. XRD patterns (Cu-Kα_1 wavelenght) of the corrosion products formed on the carbon steel immersed after 24 hours in NACE media at 35, 50 and 65 ^{o}C.

In order to establish the chemical composition of the corrosion products, after the immersion of the steel in the brine solution at different temperatures and rotation rates, it was performed the XRD characterization. Typical diffractograms recorded varying these experimental conditions are displayed in Figure 7, where is observed the signals of the substrate (Chart 96-901-3474 and 96-900-6626), magnetite (Chart 96-152-6956), feroxyhyte (Chart 96-100-8763) and sodium chloride (Chart 96-900-8679).

At the lower temperature and rotation (Figure 7a) mainly the signals related with the formation of magnetite (Fe_3O_4) are detected; which is the commonly metallic oxide reported during the oxidation of the steel [15,28,29]; meanwhile for rotations at 1000 and 2000 rpm, there are the presence of additional peaks related with the formation of feroxyhyte (δ-FeOOH). The formation of both magnetite and feroxyhyte also are observed at 65 ^{o}C varying the rotation of the electrode (Figure 7c); meanwhile at 50 ^{o}C only the signal of this oxy-hydroxide is recorded, however is expected the formation of magnetite too. The formation of δ-FeOOH is likely related with the diffusion of interstitial iron ions through the oxide which can be easily transported and precipitated at the film – solution interface. The intensity of the signals detected by XRD could be different depending on the thickness of the corrosion films which is modified by the rotation of the electrode.

Based on these results the oxidation of the steel proceeds via the formation of magnetite which is widely known being protective and adherent to the surface [28,29]. This oxide can be further oxidized raising the precipitation of feroxyhyte on the steel immersed in the media. This oxy-hydroxide had shown a less protective behavior because is partially removed by influence of the rotation of the electrode. These transitions in the chemical composition of the films could be explained depending on the oxidation of the steel; being moderate at 35 ^{o}C and aggressive for 50 and 65 ^{o}C (see Figure 1). This fact could explain the variations in the open circuit potentials shown in Figure 2 and the variation in the impedance values for 50 and 65 ^{o}C (see Figures 4 and 5). In the other hand it is observed the presence of different peaks indicating the precipitation of NaCl during the tests. It is likely to consider that this salt is trapped beneath deposits during the rotation of the electrode.

4. CONCLUSIONS

In this work the characterization of the carbon steel immersed in an aerated NACE brine varying the temperature (35, 50 and 65 ^{o}C) and the rotation rate (200, 1000 and 2000 rpm) is carried out using the rotating cylinder electrode configuration. These corrosion studies were performed by Weight Loss, EIS and XRD techniques. In the former is observed an increase in the oxidation rate of the steel as a function of the temperature and rotation rate. This active oxidation of the steel is evident in the EIS diagrams at 50 and 65 ^{o}C and 1000 and 2000 rpm; being observed a decrease in the impedance and/or phase angles values. Meanwhile by XRD technique is recorded the signals of the magnetite and feroxyhyte on the steel surface. The formation of this oxy-hydroxide by precipitation is partially removed with the rotation; enhancing the active dissolution of the carbon steel.

ACKNOWLEDGMENTS
R. Cabrera-Sierra acknowledges to CONACyT for the grant obtained to conduct his sabbatical year, and support from IPN-ESIQIE.

References

1. E. Abelev, T. A. Ramanarayanan and S. L. Bernasek, *J. Electrochem. Soc*., 156 (2009) C331.
2. A. Hernández-Espejel, M. A. Domínguez-Crespo, R. Cabrera-Sierra, C. Rodríguez-Meneses, E. M. Arce-Estrada, *Corros. Sci.*, 52 (2010) 2258.
3. M. Finšar, J. Jackson, *Corros. Sci.*, 86 (2014) 17.
4. J. A. Carew, A. Al-Sayegh and A. Al-Hashem, Paper No. 00061, *Corrosion* NACE 2000.
5. U. Osokogwu, E. Oghenekaro, *Int. J. Sci. & Tech. Res*., 1 (2012) 19.
6. M. M. Boris, Y. F. Alla, A. K. Margarita, Paper 0957, *Corrosion NACE* 2009.
7. S. Papavinasam, R. W. Revie, and M. Attard, Paper 01061, *Corrosion NACE* 2001.
8. S. Papavinasam, R. W. Revie, M. Attard, A. Demoz, J. C. Donini, and K. Michaelian, Paper 00055, Corrosion NACE 2000.
9. NACE 1D 182. Wheel Test Method Used for Evaluation of Film-Persistent Corrosion Inhibitors for Oilfield Applications.
10. ASTM G1-03 (Reapproved 2011). Standard practice for preparing, cleaning, and evaluating corrosion test specimens. ASTM International.
11. B. A. Boukamp, "Users Manual Equivalent Circuit, vers. 4.51, Faculty of Chemical Technology, University of Twente, The Netherlands,1993.
12. H. Vedage, T. A. Ramanarayaran, J. D. Munford, S. N. Smith, *Corrosion*, 49 (1993) 114.
13. R. Cabrera-Sierra, E. Sosa, M. T. Oropeza, I. González, *Electrochim. Acta*, 47 (2002) 2149.
14. J. Marín-Cruz, R. Cabrera-Sierra, M. A. Pech-Canul, *J. Sol. Sta. Electrochem.*, 11 (2007) 1245.
15. L. J. Cosmes López, E. Arce, J. Torres, J. Vazquez-Arenas, J. M. Hallen, and R. Cabrera-Sierra, *Corrosion*, 67 (2011) 116001-1.
16. A. F. Bonnel Dabosi, C. Deslouis, M. Duprat, M. Keddam, B. Tribollet, *J. Electrochem. Soc*., 130 (1983) 753.
17. M. Sancy, Y. Gourbeyre, E. M. M. Sutter, B. Tribollet, *Corros. Sci.*, 52 (2010) 1222.
18. C. Qiu, M. E. Orazem, *Electrochim. Acta*, 49 (2004) 3965.
19. X. Jiang, Y.G. Zheng, D.R. Qu, W. Ke, *Corros. Sci.*, 48 (2006) 3091.
20. D. D. Macdonald, S. R. Biaggio, H. Song, *J. Electrochem. Soc*., 139 (1992) 170.
21. E. Sikora, D. D. Macdonald, *J. Electrochem. Soc*., 147 (2000) 4087.
22. L. M. Quej-Aké, R. Cabrera-Sierra, E. M. Arce-Estrada, J. Marín-Cruz, *Int. J. Electrochem. Sci.*, 8 (2013) 924.
23. P. Bai, S. Zheng, C. Chen, *Mater. Chem. Phys.*, 149-150 (2015) 295.
24. R. Cabrera-Sierra, M. A. Pech-Canul and I. González, *J. Electrochem. Soc.*, 153 (2006) B101.
25. R. Cabrera-Sierra, J. M. Hallen, J. Vazquez-Arenas, G. Vázquez, I. González, *J. Electroanal. Chem.*, 638 (2010) 51.
26. D. D. Macdonald and S. I. Smedley, *Electrochim. Acta*, 35 (1990) 1949.
27. I. Frateur, C. Deslouis, M. E. Orazem, B. Tribollet, *Electrochim. Acta*, 44 (1999) 4345.
28. A.J. Davenport, M. Sansone, *J. Electrochem. Soc.*, 142 (1995) 725.
29. K. Daub, X. Zhang, L. Wang, Z. Qin, J.J. Noël, J. C. Wren. *Electrochim. Acta*, 56 (2011) 6661.